

**Fig. 31:** Static structure factor  $S(Q)$  of  $a\text{-CO}_2$ . **a)** and **b)**: computer simulated  $S(Q)$  for  $\text{CO}_4$  (*ab initio* molecular dynamics) and higher (classical molecular dynamics), up to octahedral, carbon coordination, respectively; **c)**, **d)** and **e)**: temperature quenched samples. The structure factor of sample (e) has been measured by decreasing pressure. The experimental  $S(Q)$  of  $a\text{-SiO}_2$  is also reported at 42 GPa (dotted line) and 28 GPa (dashed line). Symbols indicate diffraction peaks of: (stars) rhenium gasket, (squares) phase V (the closest line to peak A of  $a\text{-CO}_2$ ), and (triangles) phase III. Inset: picture of *ab initio* simulated  $a\text{-carbonia}$ .

peak (B) positioned at higher  $Q$ . The theoretical  $S(Q)$ , calculated on a fully tetrahedral atomic structure obtained by first-principle molecular dynamics [2], reproduces both experimental peaks A and B. We also compare the  $S(Q)$  of  $a\text{-carbonia}$  to that of  $a\text{-SiO}_2$ : peaks A of the two materials are close to each other, while differences in the overall profile can mainly be ascribed to the different atomic form factors.

We notice that peak A is very close to the strongest Bragg peak of crystalline  $\text{CO}_2\text{-V}$ , whose intensity has been suggested to be enhanced by disorder, indicating once again that  $a\text{-CO}_2$  is the amorphous counterpart of phase V. Upon decreasing pressure below 16 GPa,  $a\text{-CO}_2$  transforms into a new amorphous material, whose diffraction features appear to be related to the strongest Bragg peaks of phase III, and which we suggest to be the amorphous molecular counterpart of

phase III. Below 10 GPa phase I (dry ice) is formed by recrystallisation of the amorphous material.

With the discovery of “ $a\text{-carbonia}$ ”, a new, extended analogy emerges between the structures of  $\text{CO}_2$  and those of the known  $\text{SiO}_2/\text{GeO}_2$  polymorphs. Our findings lead to the general conclusion that the class of archetypal network-forming disordered systems as  $a\text{-silica}$ ,  $a\text{-germania}$ ,  $a\text{-Si}$ ,  $a\text{-Ge}$ , and water, must be extended to include  $a\text{-CO}_2$ .

## References

- [1] M. Santoro, and F. A. Gorelli, *Chem. Soc. Rev.* **5**, 918 (2006).
- [2] S. Serra, C. Cavazzoni, G. L. Chiarotti, S. Scandolo, and E. Tosatti, *Science* **284**, 788 (1999).

## Principal Publication and Authors

M. Santoro (a,b), F.A. Gorelli (a,b), R. Bini (a,c), G. Ruocco (b,d), S. Scandolo (e) and W. Crichton (f), *Nature* **441**, 857 (2006).

(a) LENS, Sesto Fiorentino (Italy)

(b) CRS-SOFT-INFM-CNR, c/o Università di Roma “La Sapienza” (Italy)

(c) Dipartimento di Chimica dell’Università di Firenze, Sesto Fiorentino (Italy)

(d) Dipartimento di Fisica, Università di Roma “La Sapienza” (Italy)

(e) ICTP and CRS-DEMOCRITOS-INFM-CNR, Trieste (Italy)

(f) ESRF

## Spatiotemporal reaction kinetics probed by picosecond X-ray diffraction

Structural dynamics in the solution phase, the environment most relevant to biology and industrial chemistry, are quite complex due to the presence of solvent molecules near solute molecules. Typically solute molecules are dissolved in the ocean of solvent molecules and complex solvation cage structures are formed. Sometimes the photo-reacted atoms or molecules can be trapped inside the cage and recombine with each other (geminate recombination). In another case, the reacted species can escape from the cage and recombine with others from other cages (non-geminate recombination). Historically, time-resolved optical spectroscopy methods have provided ample information about such processes. However, more insight into the dynamics of molecular structure in solution can be obtained using time-resolved X-ray diffraction. It was recently demonstrated that the

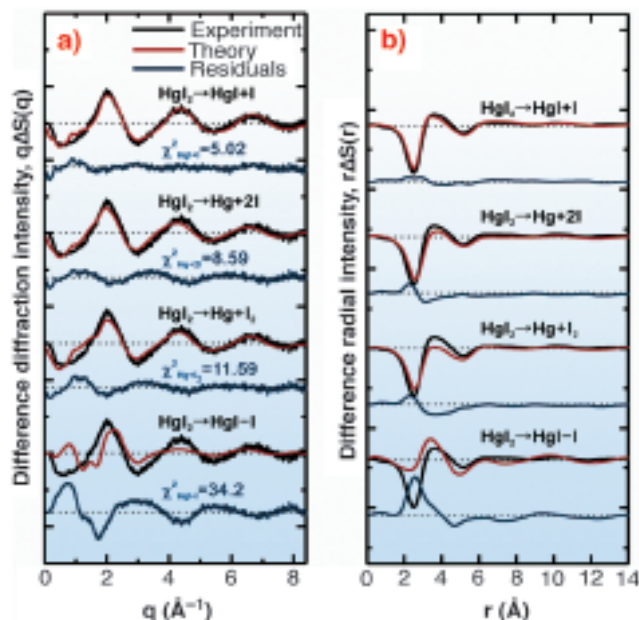


**Fig. 32:** Determination of primary photodissociation pathway of  $\text{HgI}_2$  in methanol solution. The experimental difference curves in  $q$  (a) and  $r$  space (b) at 100 ps are compared with theoretical curves using four possible putative primary pathways. The channel of two-body dissociation ( $\text{HgI}_2 \rightarrow \text{HgI} + \text{I}$ ) gives the best fit.

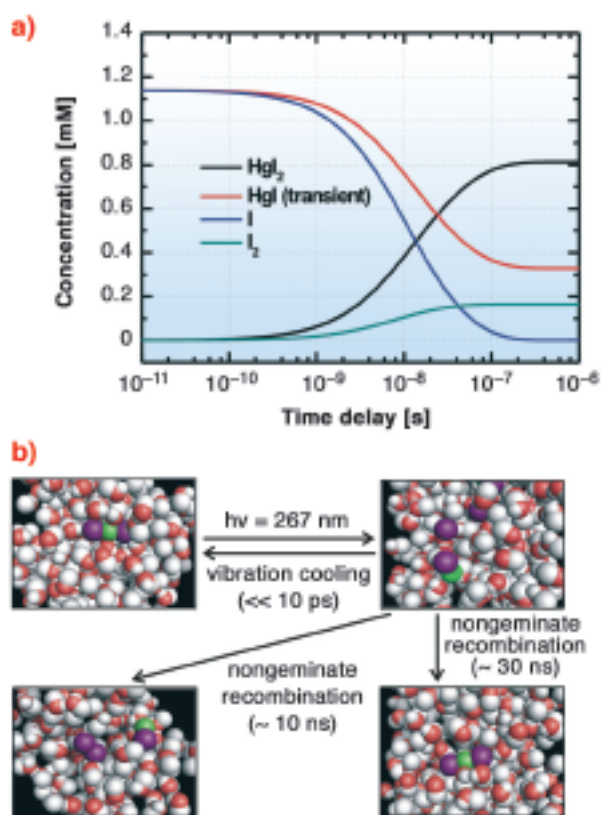


**Fig. 33:** Spatiotemporal reaction kinetics determined by time-resolved X-ray diffraction. a) The population changes of chemical species in the photodissociation of  $\text{HgI}_2$  in methanol solution. b) A schematic reaction mechanism of  $\text{HgI}_2$  photodissociation in methanol solution.

transient structure in solution can be determined by using time-resolved liquid X-ray diffraction [1].

In this work, 100 ps time-resolved liquid diffraction experiments on the photoreactions of diiodomercury ( $\text{HgI}_2$ ) dissolved in methanol (10 mM) were performed at beamline **ID09B**, using the optical pump and X-ray probe method. This molecular system has been investigated using the same technique as before, but the transient pathway and subsequent structural dynamics have not been elucidated due to the poor signal-to-noise ratio and limited data analysis method [2]. An optical pulse (267 nm, 2 ps, 986 Hz) triggers impulsive photodissociation of  $\text{HgI}_2$ , followed by subsequent reactions and then the X-ray pulse (100 ps, 0.067 nm, 986 Hz) interrogates the reacting sample by making the diffraction patterns on the CCD detector in a stroboscopic manner for the different time-delays spanning from 100 picosecond to 1 microsecond. The difference diffraction and corresponding radial intensities were extracted from the diffraction pattern and analysed using the so-called “*global-fitting method*” which considers time-dependent changes of solute and cage structures and changes of solvent structure, itself due to the time-dependent heat and density changes. Among four putative primary reaction channels (Figure 32), a two-body dissociation channel is the dominant dissociation pathway. After this primary bond fission, two parallel recombination processes proceed. Transient intermediate,  $\text{HgI}$ , associates with an iodine atom to form  $\text{HgI}_2$  nongeminately, and  $\text{I}_2$  is formed by nongeminate recombination of two iodine atoms (Figure 33) in several tens of nanoseconds. In the present work, we could clearly show two main conclusions. (1) The determination of transient species in solution is strongly correlated with solvent energetics, which depend on putative reaction channels due to the heat transfer to the solvent. Time-resolved X-ray diffraction can serve as an ultrafast calorimeter in addition to being a sensitive structural probe. (2) A manifold of structural channel can be resolved at the same time with high-precision measurement and global analysis.

Even if there are some limitations, time-resolved X-ray diffraction has matured sufficiently to provide the structure of the intermediates, correlation with solvent environment, and bulk properties of the solvent molecules in solution with unprecedented spatial and time resolution. The success of this work should stimulate future research using such outstanding capabilities for unravelling the structural dynamics of nanomaterials and proteins in the solution phase using time-resolved X-ray diffraction.

## References

- [1] H. Ihee, M. Lorenc, T.K. Kim, Q. Y. Kong, M. Cammarata, J.H. Lee, S. Bratos, and M. Wulff, *Science* **309**, 1223 (2005).

[2] A. Geis, M. Bouriau, A. Plech, F. Schotte, S. Techert, H.P. Trommsdorff, M. Wulff, and D. Block, *J. Luminescence* **94**, 493 (2001).

### Principal Publication and Authors

T.K. Kim (a), M. Lorenc (b), J.H. Lee (a), M. Lo Russo (b), J. Kim (a), M. Cammarata (b), Q.Y. Kong (b), S. Noel (b), A. Plech (c), M. Wulff (b), and H. Ihee (a), *Proc. Natl. Acad. Sci. USA* **103**, 9410 (2006).

(a) Department of Chemistry and School of Molecular Science (BK21), Korea Advanced Institute of Science and Technology (KAIST) (Republic of Korea)

(b) ESRF

(c) Fachbereich Physik der Universität Konstanz (Germany)

## New scientific opportunities at ID11

Most materials occurring in nature such as rocks, ice and soil appear as complex heterogeneous and hierarchical aggregates of crystallites, domains and dislocation structures. Man-made materials from synthetic products to engineering materials are also usually polycrystalline and inhomogeneous, as are drugs and trace particles relevant to environmental matters as well as objects of artistic or archaeological significance. Furthermore, it is a general principle that many species with high chemical activity and/or interesting mechanical properties tend to be small grained and highly defective. Examples are metal hydrides, catalysts, battery materials, and nano-grained metals.

As materials science is a field in which we try to “bring the experiment to the sample”, rather than the inverse, our goal is to obtain high quality crystallographic and micro-structural data on even these defective samples. Ultimately, we aim to perform *total simultaneous hierarchical characterisation* (Figure 34) of arbitrary samples. To this end, we have developed an array of new diffraction-based methods based on high-energy microfocussing called three-dimensional X-ray diffraction (3DXRD) microscopy, to characterise polycrystalline samples over several length scales, from the Ångström scale (crystal structure) to the grain

distribution over the entire sample (see [1] for a recent review).

The sub-micrometre range is of particular interest in materials science as it is the critical length scale for many inter-granular interactions such as dislocations, cracks and interfaces; it is these interactions which ultimately give rise to the bulk properties of materials. The lack of a detailed knowledge of the distributional heterogeneity of properties on this scale has resulted in our inability to construct rigorous first-principles models of such basic materials properties as strength, fatigue resistance, and texture development. This length scale is also crucial in the microelectronics industry, where many features on modern chips are below 100 nm.

To study such features, bulk information may be collected by powder diffraction, but such data represents an ensemble average of the sample grains, and is uninformative on sample inhomogeneity, inter-granular interactions and the form of distributions of properties. Electron microscopy data has high spatial and angular resolution, but is limited to surfaces and static measurements. 3DXRD thus acts as the bulk equivalent of an electron microscope, acquiring spatial and structural data in the sub-micrometre scale in bulk samples in real time.

ID11 was one of first beamlines to open at the ESRF, and has been continually upgraded over the last ten years to take advantage of emerging technology and follow trends in materials science research. The development of 3DXRD on ID11 led to the construction of a dedicated station for high-energy microfocussing in the late 1990s. Due to the growing interest in these techniques, a new station has been built in order to extend this effort into the domain of high-energy nano-focussing. At the beginning of 2007, this outstation will become the first of the second wave of long beamlines at the ESRF open for the user programme.

With the present 3DXRD microscope, the spatial resolution is  $\sim 5 \mu\text{m}$ , while grains of 150 nm can be observed. The extension project aims to allow us to obtain sub-micrometre mapping resolution, with transverse resolutions below 100 nm and sensitivity to the earliest stages of nano-crystallisation. In order to

**Fig. 34:** Characterisation of a sample on several length scales: from the distribution of grains (left) to the crystal and molecular structures via 3DXRD.

